# Battery Thermal Behavior in Hybrid Energy Storage Unit (Battery / Supercapacitor) for Dynamic Loads

Si Mohamed FARESSE, Mohamed ASSINI, Abdellah SAAD

**Abstract** — This work consists in studying thermal behavior of classical electrical energy storage (batteries), hybrid (batteries / supercapacitors) and controlled hybrid system. We will use in this study a Lithium-Ion battery, an electrochemical double layer supercapacitor and a variable Load, that corresponds to electrical vehicles dynamic operation, to illustrate the performance of these storage units. Under Matlab / Simulink environment will be treated classical, hybrid followed by controlled hybrid system. The results obtained by simulation confirm the interest of integrating supercapacitors into a battery-based electrical energy storage system. The controllable hybrid storage unit also made it possible to relieve batteries perfectly and to protect them from high temperature level.

**Index Terms**— Battery, Supercapacitor, Hybrid Storage, Thermal Behavior, Electric Vehicle, Energy Storage Control System.

———————————————— ◆ ————————————————

## 1 INTRODUCTION

Electrical energy storage technologies are very diverse, depending on the nature of the needs and the kind of applications [1]. Especially, electric vehicles require on-board storage solutions, intelligent and able to ensure a good quality of energy [2]. This induces the response to the varying needs of the drive chain and essentially the ability to provide electrical power peaks of starting, acceleration and deceleration [3].

Conventional energy storage systems for electric vehicles use generally batteries, which rely mainly on the conversion of chemical to electrical energy [4]. But the batteries have too slow dynamic and don't support high power fluctuations, as this will negatively affect their performance [5].

The use of supercapacitors (SC) as a complementary storage element to batteries is a technique adapted to applications that require a rapid exchange of power demand and a large storage capacity [6]. In recent years, this storage technique is the subject of research activity through numerous scientific programs.

The hybrid storage topologies Batteries-Supercapacitors are various, and they depend particularly on the type of use [7]. For the studied case we have selected a parallel topology which consists in using a DC / DC converter to separate the batteries from the DC bus, and to connect the supercapacitor pack directly on the DC bus (Fig. 1), this choice makes it possible to ensure better efficiency in terms of cost, weight and power control [8].

Such a configuration reflects an optimization of energy transfer, since it makes it possible to show the interest of hybridization [9], its positive impact to maintain battery performance, and to meet the needs of applications that require a rapid response to variations and load peaks [10].

In the present work, we will study, modelize and simulate under Matlab / Simulink environment a hybrid storage based on batteries and supercapacitors, in which we are only interested in the energy exploitation phase, to illustrate thermal behavior of the battery against dynamic loads.

This paper is organized as follows : After Introduction is given in the first section, the system description and modeling are presented in Section 2. The study of electrical equivalent circuit of the system is dressed in Sections 3. Section 4 introduces a proposed data for simulation and the DC Bus control method. Section Simulation Results and Discussion elaborate the thermal performance analysis of the combinaison battery and supercapacitor. Conclusions are given in the last section.

## 2 ENERGY STORAGE SYSTEM DESCRIPTION AND MODELING

### 2.1 Energy Storage System Description

The main parts of this storage system are : the battery that can provide high energy but lower power density and the supercapacitor that can deliver high power but lower energy density [11]. This hybrid storage unit is feeding a dynamic load. The battery is connected to the bus through a DC / DC converter and the supercapacitor is directly connected to this bus. This is the parallel topology, which can only provides the control of the battery. The supercapacitor is responding instanuously.



Fig. 1 Parallell Topology Energy Storage System
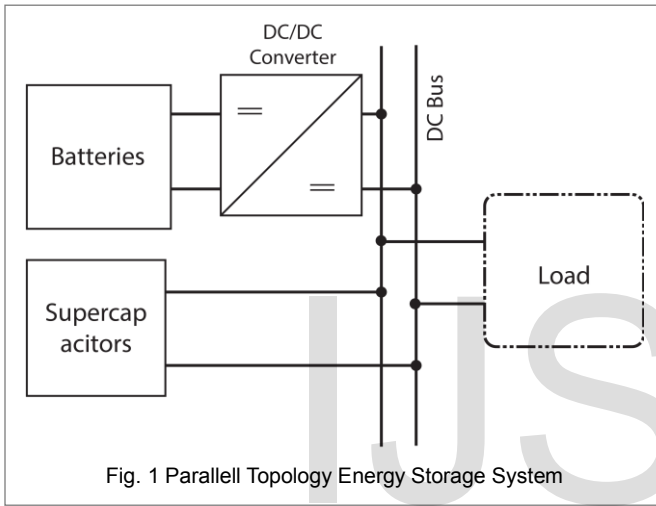
### 2.2 Battery Model

In this work, we use Matlab Model for lithium-ion battery. Two models will be presented below (with and without tempearature effect). For each model the discharge equation will be presented. The lithium-ion battery model without temperature effect is given as [12] :

$$V_{batt}(it, i^*, i) = E_0 - K\frac{Q}{Q - it}.i^* - K\frac{Q}{Q - it}.it$$
$$+A.\exp(-B.it) - R_b.i \qquad (1)$$

The impact of temperature on the model parameters is represented bellow [13,14] :

$$V_{batt}(it, i^*, i, T, T_a) = E_0(T) - K(T)\frac{Q(T_a)}{Q(T_a) - it}.(i^* + it)$$
$$+A.\exp(-B.it) - C.it - R_b(T).i \qquad (2)$$

With :

$$E_0(T) = E_0|_{T_{ref}} + \frac{\partial E}{\partial T}(T - T_{ref}) \qquad (3)$$

$$K(T) = K|_{T_{ref}}.\exp(\alpha.(\frac{1}{T} - \frac{1}{T_{ref}})) \qquad (4)$$

$$Q(T_a) = Q|_{T_a} + \frac{\Delta Q}{\Delta T}(T_a - T_{ref}) \qquad (5)$$

$$R_b(T) = R_b|_{T_{ref}}.\exp(\beta.(\frac{1}{T} - \frac{1}{T_{ref}})) \qquad (6)$$

The cell or internal temperature T, at any given time t, is expressed as :

$$T(t) = L^{-1}(\frac{P_{loss}R_{th} + T_a}{1 + s.t_c}) \qquad (7)$$

Where :

$$P_{loss} = (E_0(T) - V_{batt}(T)).i + \frac{\partial E}{\partial T}.i.T \qquad (8)$$

### 2.3 Supercapacitor Model

The supercapacitor is an emerging technology in the field of energy storage systems. Energy storage is performed by the means of static charge rather than of an electro-chemical process that is inherent to the battery [15,16,17]. The Supercapacitor model used in this work is a Generic Matlab Model parameterized to represent most popular types of supercapacitors [18,19]. The supercapacitor output voltage is expressed using a Stern equation as:

$$V_{sc} = \frac{N_s Q_T d}{N_p N_e \varepsilon \varepsilon_0 A_i}$$
$$+\frac{2N_e N_s RT_o}{F} sinh^{-1}(\frac{Q_T}{N_p N_e^2 A_i \sqrt{8RT_o \varepsilon \varepsilon_0 c}}) - R_{sc}.i_{sc} \qquad (9)$$

With : $Q_T = \int i_{sc}\, dt$

## 3 SIMPLIFIED ELECTRIC CIRCUIT OF HYBRID ENERGY STORAGE SYSTEM

In this section, the electrical circuit is studied in order to establish the current ratio contribution for each component in the system. Because, the current is the main temperature cause of the battery [20].

### 3.1 Electrical Equivalent Circuit

We consider the following simplified equivalent electrical circuit:



Fig. 2 Hybrid Energy Storage Equivalent circuit
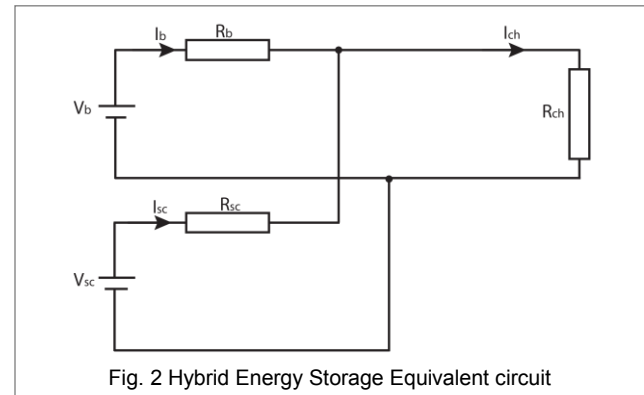
The battery and supercapacitor are considered in this study as ideal voltage sources in series with their internal resistors.

## 3.2 System Characteristics

Thevenin Equivalent parameters of the circuit in Fig. 2 are :

$$R_T = R_b \; // \; R_{sc} \; = \frac{R_b \cdot R_{sc}}{R_b \; + \; R_{sc}} \qquad (10)$$

$$V_T = \frac{V_b/R_b \; + \; V_{sc}/R_{sc}}{1/R_b \; + \; 1/R_{sc}} = \frac{R_{sc} \cdot V_b \; + \; R_b \cdot V_{sc}}{R_b \; + \; R_{sc}} \qquad (11)$$

The circuit can be modeled by the following equation:

$$\begin{bmatrix} R_b \; + \; R_{ch} & R_{ch} \\ R_{ch} & R_{sc} \; + \; R_{ch} \end{bmatrix} \begin{bmatrix} I_b \\ I_{sc} \end{bmatrix} = \begin{bmatrix} V_b \\ V_{sc} \end{bmatrix} \qquad (12)$$

Currents are then :

$$I_b = \frac{(R_{sc} \; + \; R_{ch}) \cdot V_b \; - \; R_{ch} \cdot V_{sc}}{R_b \cdot R_{sc} + (R_b \; + \; R_{sc}) \cdot R_{ch}} \qquad (13)$$

$$I_{sc} = \frac{(R_b \; + \; R_{ch}) \cdot V_{sc} \; - \; R_{ch} \cdot V_b}{R_b \cdot R_{sc} + (R_b \; + \; R_{sc}) \cdot R_{ch}} \qquad (14)$$

Bus Voltage is given by :

$$V_{bus} = \frac{V_b/R_b \; + \; V_{sc}/R_{sc}}{1/R_b \; + \; 1/R_{sc} + 1/R_{ch}} \qquad (15)$$

## 3.3 Maximal Load Calculation

If $R_{ch} = R_T$, we have a maximum transfer of power given by :

$$P_{max} = \frac{V_T^2}{4R_T} = \frac{(R_{sc} \cdot V_b \; + \; R_b \cdot V_{sc})^2}{4 \; R_b \; R_{sc} \; (R_b \; + \; R_{sc})} \qquad (16)$$

## 3.4 Supercapacitor Contribution Ratio

The supercapacitor current contribution ratio is given by :

$$\begin{aligned} \alpha_{sc}(\%) &= \frac{I_{sc}}{I_{sc} \; + \; I_b} \\ &= \frac{(R_b \; + \; R_{sc}) \cdot V_{sc} + R_{ch} \cdot V_b}{(R_b \; + \; 2R_{sc}) \cdot V_{sc} + (R_{sc} \; + \; 2R_{sc}) \cdot V_b} \cdot 100 \end{aligned} \qquad (17)$$

## 4  SIMULATION DATA AND DC BUS LOGIC CONTROL

In a storage energy system, the sizing of the various elements (batteries, supercapacitors and converters) is carried out according to the predictions of the desired autonomy and the power demanded by the load [21]. The goal of our study is not the sizing of the storage unit, but to study its behavior. In our case study, the DC bus voltage is fixed to 12.6V. The load that has been selected allows the simulation of the behavior of the motors during start-up and during nominal operation.

### 4.1 System Case study

For our case study, the battery, supercapacitor and the load are chosen as follow :

TABLE 1
BATTERY PARAMETERS

| Parameters | Value |
| --- | --- |
| Nominal Voltage | 12.6  V |
| Rated capacity | 40 Ah |
| Initial state-of-charge | 100 % |
| Battery response time | 30s |
| Cut-off Voltage | 10.5 V |
| Fully charged voltage | 13.8 V |
| Nominal discharge current | 20 A |
| Internal resistance | 15e-3 Ohm |
| Capacity at nominal voltage | 30.14 Ah |
| Exponential zone Voltage | 13.1 V |
| Exponential zone Capacity | 0.5 Ah |
| Initial cell temperature | 20 °C |
| Nominal ambiant temperature | 20 °C |
| Thermal resistance, cell-to-ambient | 0.6411 °C/W |
| Thermal time constant, cell-to-ambient | 4880 s |
| Permissible discharge temperature | −20 to 60 °C |

TABLE 2
SUPERCAPACITOR PARAMETERS

| Parameters | Value |
| --- | --- |
| Rated capacitance | 10e4 F |
| Equivalent DC serie resistance | 1e-3 Ohm |
| Rated voltage | 12.6 V |
| Number of series capacitors | 5 |
| Number of parallel capacitors | 2 |
| Initial voltage | 13.8 V |
| Operating temperature | 25 °C |
| Number of layers | 1 |
| Molecular radius | 1e-9 m |
| Permittivity of electrolyte material | 6.0208e-10 F/m |

**Load Characteristics :**

The load that has been selected allows the simulation of the behavior of the motors during start-up and during nominal operation, acceleration and deceleration. The nominal current has been chosen equal to 40A and the maximum current to 400A.

### 4.2 The control logic of the system

Our goal is to keep the bus voltage at the reference value and the battery temperature within the allowable limits. In order to do so, we propose to control the battery current contribution to its nominal value when the supercapacitor is able to provide the load demand. If the supercapacitor is discharged we remove the current limitation of the battery and we monitor its temperature, if it reaches the maximum level we disconnect the load.

## 5 SIMULATION RESULTS AND DISCUSSION

The system is implemented in Matlab/Simulink environment that provide a simulation platform through the integration of the transfer functions or the implementation of the physical elements with SimPowerSytems library.
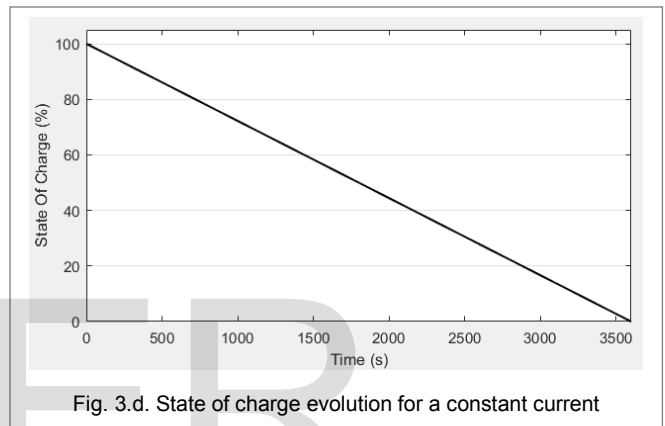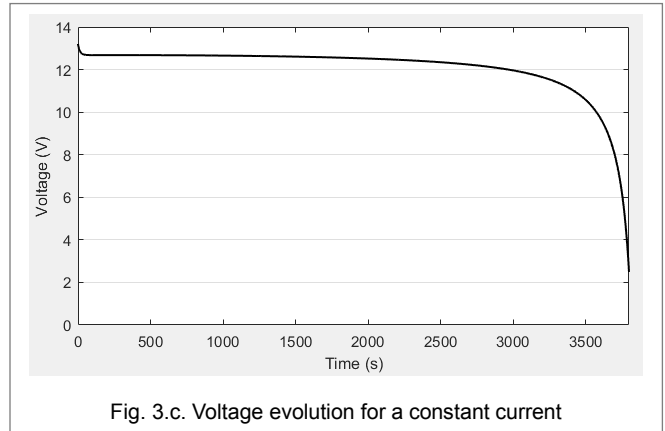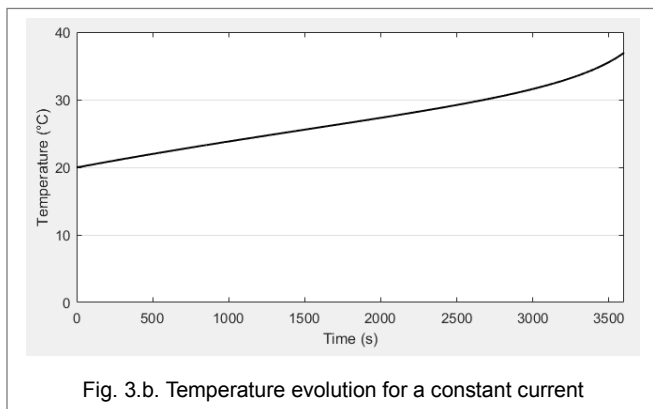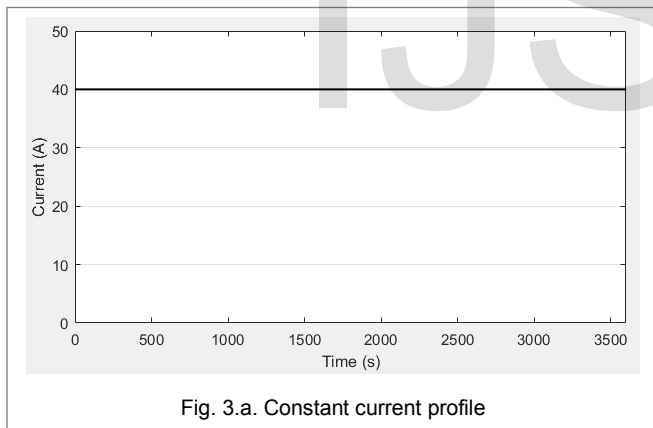
In order to analyze the battery behavior, the simulation tests were performed with different operating conditions. We proposed three simulation tests that represent battery thermal behavior in classical, hybrid and controlled hybrid energy storage system. To explain the interest of adding a supercapacitor to a conventional energy storage system, its contribution is presented in the last part of this section. For all simulations, the battery and supercapacitor are assumed initially charged.

### 5.1 Battery Behavior Analysis

Battery temperature evolution has been simulated with two load profiles (constant and dynamic). The simulation time was chosen so that it is equal to battery discharge time.

**Constant Load Profile :**

For a constant current draw equal to 40 A, the battery full discharge time is about 3600 seconds. Battery parameters evolution is given in Fig. 3 (a-d).



Fig. 3.a. Constant current profile



Fig. 3.b. Temperature evolution for a constant current



Fig. 3.c. Voltage evolution for a constant current



Fig. 3.d. State of charge evolution for a constant current

For this simulation, temperature rises from ambient 20 °C to 37 °C after one hour of operation. It stays within the permissible limits. We also notice that there is no voltage drop. This load profile represents a normal and favorable operating regime for the battery.

**Dynamic Load Profile :**

To simulate a dynamic regime, the current draw goes from 40 A to 400 A repeatedly. During 700 seconds, the total discharge time of the battery, the results obtained are given in Fig. 4 (a-d).


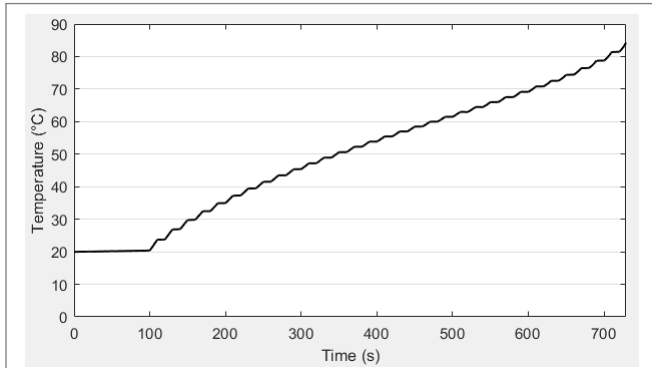
Fig. 4.a. Dynamic current profile
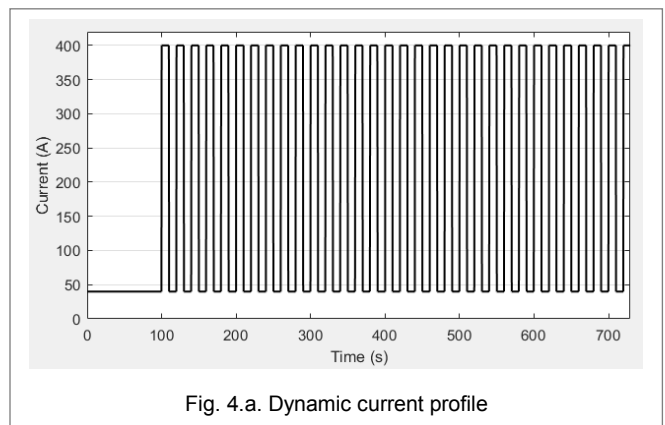
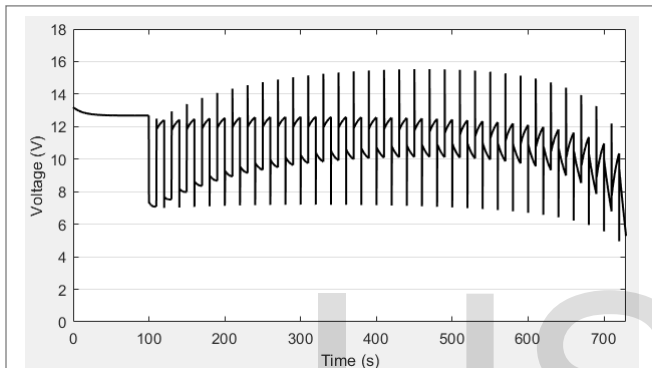Fig. 4.b. Temperature evolution for a dynamic current
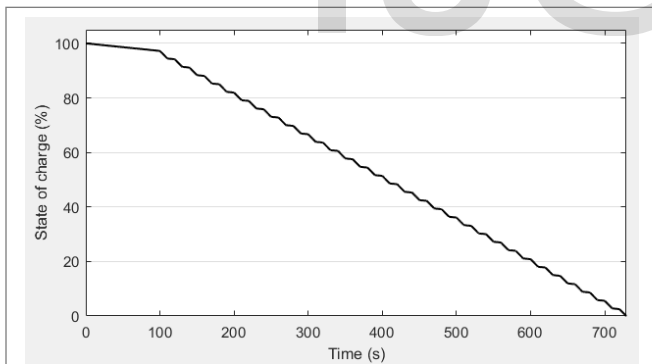


Fig. 4.c. Voltage evolution for a dynamic current



Fig. 4.d. State of charge evolution for a dynamic current

For this load profile, the allowable temperature limit is reached after 500 seconds. This temperature is constantly evolving to reach 90 °C at 700 seconds.

We also notice that there is a large voltage drop of about 40% compared to the reference voltage. This load profile represents the critical regime that can bring the battery out of its normal operation.

## 5.2 Battery and Supercapacitor Behavior Analysis

According to section 5.1, we notice that the battery is able to

supply power to applications requiring a constant current. On the other hand, variable regimes require the introduction of a power density element such a supercapacitor, which can respond quickly to high instantaneous current calls [22].

In this part we will be interested in the contribution of supercapacitors in this classic storage system. The dynamic profile load is chosen as in Fig. 4.a. Simulation results are given in Fig. 5 (a-d).
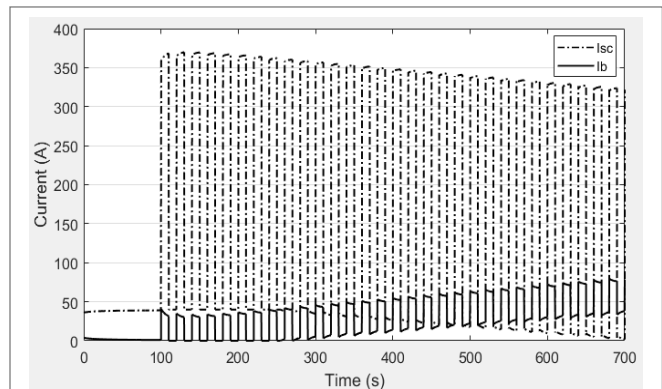


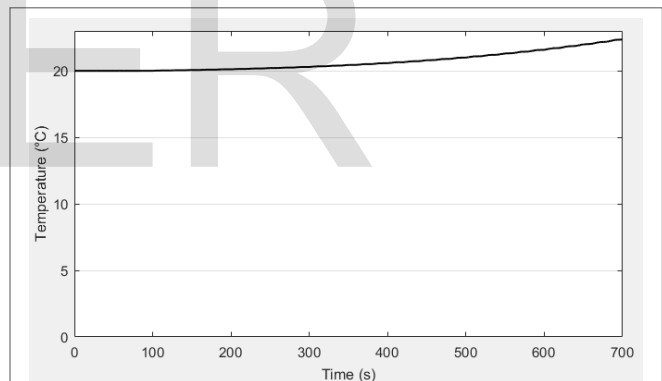Fig. 5.a. Battery and supercapacitor current contribution



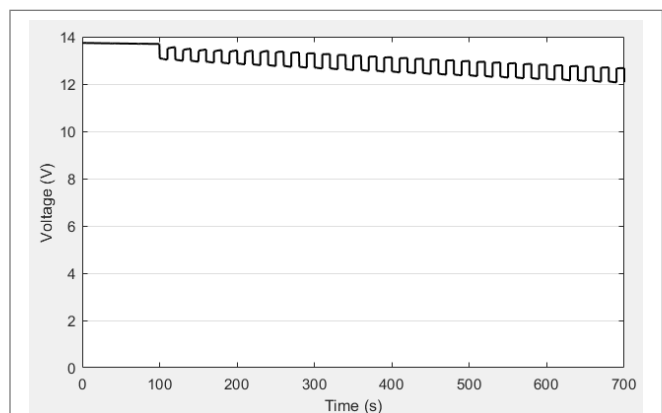Fig. 5.b. Temperature evolution for a dynamic current



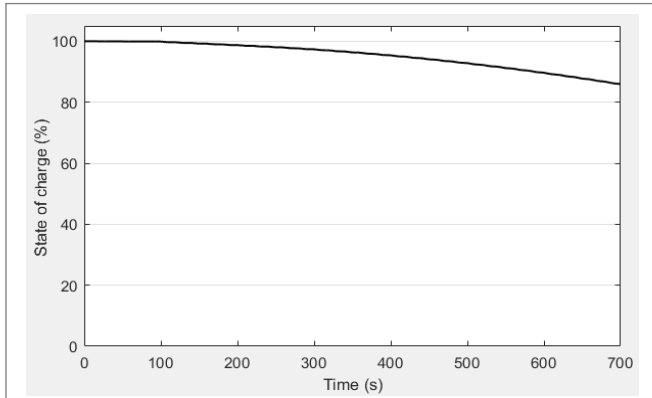Fig. 5.c. Voltage evolution for a dynamic current

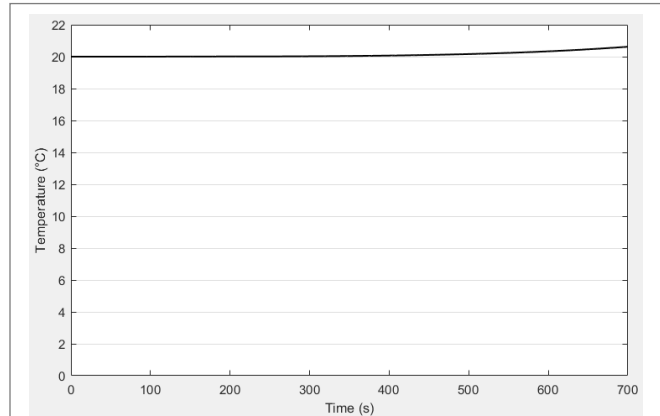Fig. 5.d. State of charge evolution for a dynamic current



Fig. 6.b. Temperature evolution for a dynamic current

According to these simulation results, there is a great performance evolution of a hybrid storage system compared to a conventional system. Despite large current draws, the battery temperature only changed by 2.5 °C after 700 seconds and the voltage drop remained almost below 5% of the reference voltage. During this kind of operation the supercapacitor assures the responses to the power demands, while the battery contributes accordingly to supplement the load current demand. The battery remains relieved and its temperature became constant. In the studied case, the supercapacitor begins to contribute by a value of 90% or 360 A. After 700 seconds, its contribution fell to 80% because of its state of charge decrease. For current calls of 400A, the contribution of the battery has continued to increase from 40 A to 80 A. In this case no current limitation was imposed to the battery.
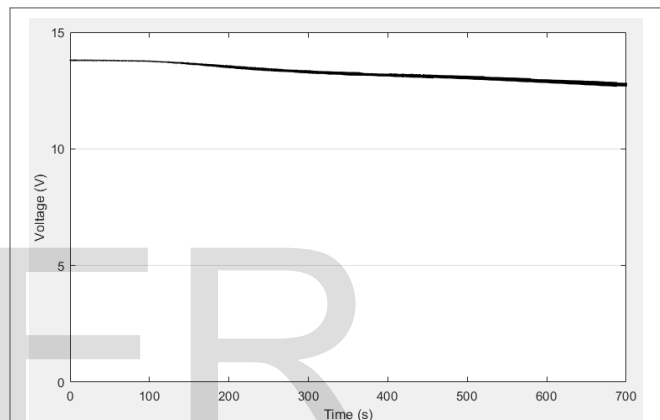
### 5.3 Battery with DC/DC Converter and Supercapacitor Behavior Analysis

Hybrid energy system with controllable DC/DC converter was simulated in order to see the improvement made by limiting current flow from the battery. The dynamic profile load is chosen as in Fig. 4.a. The voltage drop and the temperature rise are given in Fig. 6 (a-d).



Fig. 6.c. Voltage evolution for a dynamic current
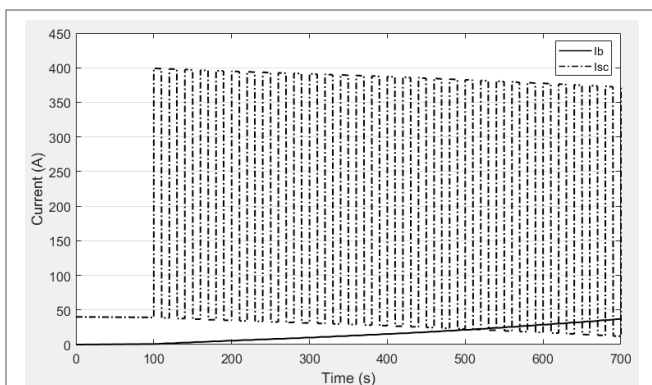


Fig. 6.a. Battery and supercapacitor current contribution
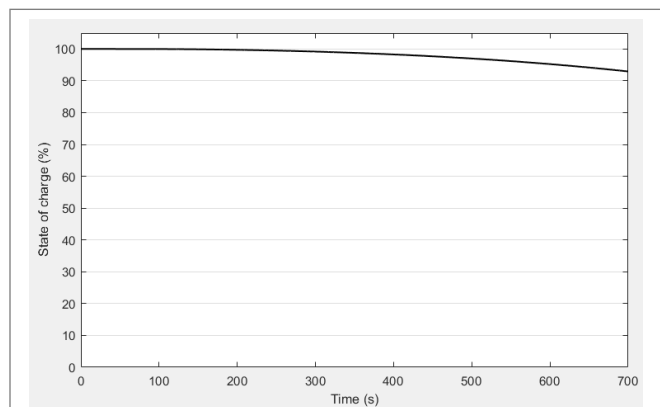


Fig. 6.d. State of charge evolution for a dynamic current

For this simulation the battery current was limited to 35A. This new storage system has further increased the performance of a hybrid system. The presence of a converter allowed us to limit the current on the one hand and on the other hand to regulate the voltage. The battery temperature changed by 0.7 °C after 700 seconds and the voltage drop remained almost below 1% of the reference voltage.

## 5.4 Battery and Supercapacitor Contribution

Referring to Section 3 equations, and considering the voltage levels of the battery and the supercapacitor equal. The equivalent electrical circuit parameters of the hybrid storage system are given in Table 3.

TABLE 3
ELECTRICAL EQUIVALENT CIRCUIT PARAMETERS

| Parameters | Values |
|---|---|
| Battery Voltage | 12.6 V |
| Supercapacitor Voltage | 12.6 V |
| Thevenin Resistance | 0.94 mΩ |
| Thevenin Voltage | 12.6 V |
| Maximum Power | 42 336 W |

The evolution of the system parameters are given in Table 4. Two cases are mentioned, namely : 40A and 400A.

TABLE 4
EVOLUTION OF SYSTEM PARAMETERS BASED ON CURRENT

| Parameters | Load Current | |
|---|---|---|
| | 40 A | 400 A |
| Load Resistance | 314.0 mΩ | 30.6 mΩ |
| Bus Voltage | 12.56 V | 12.23 V |
| Voltage Drop | 0.30 % | 2.98 % |
| Battery Current | 2.5 A | 25.0 A |
| Supercapacitor Current | 37.5 A | 375.0 A |
| Supercap. Contribution Ratio | 93.8 % | 93.8 % |

Table 4 shows that the voltage drop increases with the current draw and it is given by the following formula : $V_{bus_{ref}} - R_T.I_{ch}$. For the case studied, the voltage drop will be greater than 5% of the reference voltage for a current draw greater than 672A. We also notice that the contribution of the supercapacitor in this storage system is about 94% due to its very low internal resistance.

## 6 CONCLUSION

Battery thermal behavior in hybrid energy storage for dynamic loads is illustrated in this paper. The battery model taking into account the temperature effect has been presented. Then, to demonstrate the limitation of conventional storage system we test the battery with constant and peak power demands. We notice that the temperature reaches permissible limit and the voltage drop was high. Then, the importance of using supercapacitors for dynamic load has been elaborated. Battery temperature remains within the allowable limit, but the voltage drop is near 5%. The control of the battery current flow allowed us to remove this voltage drop.

## NOMENCLATURES

| | |
|---|---|
| $V_{batt}$ | Battery voltage (V) |
| $E_0$ | Constant voltage (V) |
| K | Polarization constant (Ah⁻¹) |
| i* | Low frequency current dynamics (A) |
| i | Battery current (A) |
| it | Extracted capacity (Ah) |
| Q | Maximum battery capacity (Ah) |
| A | Exponential voltage (V) |
| B | Exponential capacity (Ah⁻¹) |
| $R_b$ | Battery internal resistance (Ω) |
| $T_{ref}$ | Nominal ambient temperature (K) |
| T | Cell or internal temperature (K) |
| $T_a$ | Ambient temperature (K) |
| $\partial E/\partial T$ | Reversible voltage temperature coefficient (V/K) |
| α | Arrhenius rate constant for the polarization resistance |
| β | Arrhenius rate constant for the internal resistance |
| $\Delta Q/\Delta T$ | Maximum capacity temperature coefficient (Ah/K) |
| C | Nominal discharge curve slope (V/Ah) |
| $R_{th}$ | Thermal resistance, cell to ambient (°C/W) |
| $t_c$ | Thermal time constant, cell to ambient (s) |
| $P_{loss}$ | Overall heat generated during charge/discharge (W) |
| $i_{sc}$ | Supercapacitor current (A) |
| $V_{sc}$ | Supercapacitor voltage (V) |
| $R_{sc}$ | Supercapacitor total resistance (ohms) |
| $N_e$ | Number of layers of electrodes |
| $N_P$ | Number of parallel supercapacitors |
| $N_s$ | Number of series supercapacitors |
| $Q_T$ | Electric charge (C) |
| R | Ideal gas constant |
| d | Molecular radius |
| $T_o$ | Operating temperature (K) |
| ε | Permittivity of material |
| $\varepsilon_0$ | Permittivity of free space |
| $A_i$ | Interfacial area between electrodes and electrolyte (m²) |
| c | Molar concentration (mol/m³) |
| F | Faraday constant |
| $V_{bus_{ref}}$ | Bus voltage reference |
| $R_T$ | Thevenin resistance |
| $V_T$ | Thevenin voltage |
| $R_{ch}$ | Load resistance |
| $I_{ch}$ | Load current |
| $P_{max}$ | Maximal power transfer |
| $\alpha_{sc}$ | Supercapacitor contribution ratio |

## REFERENCES

[1] M.A. Camara, "Modélisation du stockage de l'énergie photovoltaïque par supercondensateurs," PhD dissertation, Université Paris Est Créteil, France, 2011.

[2] A. Castaings, W. Lhomme, R. Trigui and A. Bouscayrol, "Comparison of energy management strategies of a battery/supercapacitors system for electric vehicle under real-time constraints," *Applied Energy*, vol. 163, pp. 190-200, Feb 2016.

[3] J. Ruan, P.D. Walker, N. Zhang and J. Wu, "An investigation of hybrid energy storage system in multi-speed electric vehicle," *Energy*, vol. 140, pp. 291-306, Dec 2017.

[4] L. Kouchachvili, W. Yaïci and E. Entchev, "Hybrid battery/supercapacitor energy storage system for the electric vehicles," *Journal of Power Sources*, vol. 374, pp. 237-248, Jan 2018.

[5] K. Benabdelaziz and M. Maaroufi, "Battery dynamic energy model for use in electric vehicle simulation," *International Journal of Hydrogen Energy*, vol. 42, no. 30, pp. 19496-19503, Jul 2017.

[6] A. Lahyani, P. Venet, A. Guermaz and A. Troudi, "Battery/supercapacitors combination in uninterruptible power supply (UPS)," *IEEE Transactions on Power Electronics*, vol. 28, no. 4, pp. 1509–1522, Apr 2013.

[7] S. Sreedhar, J.B. Siegel and S. Choi, "Topology Comparison for 48V Battery-Supercapacitor Hybrid Energy Storage System," *IFAC-PapersOnLine*, vol. 50, no. 1, pp. 4733-4738, Jul 2017.

[8] N.M. Souleman, "Design and simulation of a fuel cell hybrid emergency power system for a more electric aircraft : evaluation of energy management schemes," PhD dissertation, École de technologie supérieure, Montréal, Canada, 2013.

[9] T. Ma, H. Yang and L. Lu, "Development of hybrid battery–supercapacitor energy storage for remote area renewable energy systems," *Applied Energy*, vol. 153, pp. 56-62, Sept 2015.

[10] A. Lahyani, A. Sari, I. Lahbib and P. Venet, "Optimal hybridization and amortized cost study of battery/supercapacitors system under pulsed loads," *Journal of Energy Storage*, vol. 6, pp. 222-231, May 2016.

[11] N. Mendis, K.M. Muttaqi and S. Perera, "Management of Low- and High-Frequency Power Components in Demand-Generation Fluctuations of a DFIG-Based Wind-Dominated RAPS System Using Hybrid Energy Storage," *IEEE Transactions on Industry Applications*, vol. 50, no. 3, pp. 2258–2268, May/Jun 2014.

[12] O. Tremblay and L.A. Dessaint, "Experimental Validation of a Battery Dynamic Model for EV Applications," *World Electric Vehicle Journal*, vol. 3, May 2009.

[13] L.H. Saw, K. Somasundaram, Y. Ye and A.A.O. Tay, "Electro-thermal analysis of Lithium Iron Phosphate battery for electric vehicles," *Journal of Power Sources*, vol. 249, pp. 231–238, Mar 2014.

[14] C. Zhu, X. Li, L. Song and L. Xiang, "Development of a theoretically based thermal model for lithium ion battery pack," *Journal of Power Sources*, vol. 223, pp. 155–164, Feb 2013.

[15] P.O. Logerais, M.A. Camara, O. Riou, A. Djellad, A. Omeiri, F. Delaleux and J.F. Durastanti, "Modeling of a supercapacitor with a multibranch circuit," *International Journal of Hydrogen Energy*, vol. 40, no. 39, pp. 13725-13736, Oct 2015.

[16] F. Belhachemi, "Modélisation et caractérisation des supercondensateurs a couche double électrique utilisées en électronique de puissance," PhD dissertation, Institut National Polytechnique de Lorraine, France, 2001.

[17] N. Rizoug, "Modélisation électrique et énergétique des supercondensateurs et méthodes de caractérisation: application au cyclage d'un module de supercondensateurs basse tension en grande puissance," PhD dissertation, Université de Lille, France, 2006.

[18] K.B. Oldham, "A Gouy-Chapman-Stern model of the double layer at a (metal)/(ionic liquid) interface," *Journal of Electroanalytical Chemistry*, vol. 613, no. 2, pp. 131–38, Feb 2008.

[19] N. Xu and J. Riley, "Nonlinear analysis of a classical system: The double-layer capacitor," *Electrochemistry Communications*, vol. 13, no. 10, pp. 1077–1081, Oct 2011.

[20] F. Mocera and E. Vergoria, "Study and identification of the thermo-electric behavior of lithium-ion batteries for electric vehicles," *Procedia Structural Integrity*, vol. 8, pp. 126-136, 2018.

[21] D. Paire, "Dimensionnement et gestion d'énergie de systèmes d'entraînements électriques hybrides : application à un ascenseur avec récupération d'énergie," PhD dissertation, Université de Technologie de Belfort-Montbeliard, France, 2010.

[22] Z. Cabrane, M. Ouassaid and M. Maaroufi, "Analysis and evaluation of battery-supercapacitor hybrid energy storage system for photovoltaic installation," *International Journal of Hydrogen Energy*, vol. 41, no. 45, pp. 20897-20907, Dec 2016.